

STABILITY ANALYSIS OF ASDEX-H-MODE DISCHARGES

K. Grassie, O. Gruber, O. Klüber, M. Kornherr, H.P. Zehrfeld

Max-Planck-Institut für Plasmaphysik
Association Euratom-IPP, D-8046 Garching

1. Introduction : Due to the accessibility of the H-regime, β_p values close to the Troyon limit can be achieved in ASDEX discharges with neutral particle injection at a moderate power level. In the last couple of years detailed β_p -optimization studies have been performed in a large range of values for the toroidal field ($1.2 < B_t < 2.7$ T) and plasma current ($0.2 < I_p < 0.48$ MA) with beam powers up to 4.5 MW.

In many cases a 'hard- β saturation' is observed, when β approaches β_c , i.e. after reaching its maximum value β decreases to a lower stationary level with $\beta/\beta_c \sim 0.7$. This stationary phase lasts of the order of 100 ms and is a peculiar property of ASDEX-high- β discharges — in contrast to Doublet-III, where generally a disruption occurs a couple of ms after β has reached its maximum.

Clearly it is of considerable interest to investigate the MHD activity of these discharges and compare them with theoretical calculations in order to get more insight in the physical mechanisms that govern the high- β_p phase. Our tool for this investigation is the GA-3D-CART code, which is based on the large aspect ratio expanded MHD equations at finite β . This set of equations is solved for realistic ASDEX equilibria, which have been determined by the Garching free boundary flow equilibrium code NIVA. The necessary profile information has been obtained from a detailed analysis of measured profiles by means of the PPPL code TRANSP [1,2].

For a detailed investigation of the MHD-characteristics of ASDEX-H-mode discharges we refer to O. Klüber et al. [3]; a description of the CART-code is given in Ref.[4].

2. Linear results : Typical results for the perturbed, linearized $n = 1$ magnetic flux $\psi(x,y)$ for discharges with medium β_p ($\beta_p \sim 1$) and large β_p ($\beta_p \sim 2$) are presented in Ref.[5] for constant vacuum resistivity $\eta_V = 10^{-2}$ (in rationalized emu).

We generally find that the global MHD-activity is mainly caused by tearing or pressure driven modes. External kink contributions are weak for our cases ($\Delta\tilde{\gamma} < 10\%$), as can be shown by moving the conducting wall to the plasma surface. A change in the driving mechanism for the instability with increasing pressure is indicated by the η -scaling of the growth rates. It turns out that low- β_p -discharges scale like $\eta^{3/5}$, as expected for tearing modes, whereas an interchange mode scaling $\tilde{\gamma} \sim \eta^{1/3}$ is found for high- β_p -discharges. Contour-plots of the magnetic flux show that the predicted mode activity is concentrated at the outer side of the torus and that the poloidal wavelength there is in general smaller than that at the inner side [5,6]. This behaviour is not only in contradiction with experiment, but also with the expectation based on the assumption that the main part of the perturbed current flows parallel to the equilibrium magnetic field. Then, since the field line slope is smaller at the inner side of the torus, one expects a shorter poloidal wavelength there. This discrepancy is considered a consequence of the particular treatment of toroidal effects by the reduced equations.

Another problem consists of the observation of large poloidal mode numbers, which clearly exceed the q_a value of the discharge under consideration [3]. An example is the high- β_p discharge #18041 ($\beta_p \approx 1.92$) with $q_a = 3.4$ and a measured value of $m \approx$

4, $n = 1$. It turns out that a simulation of these results with constant vacuum resistivity is impossible. This problem can be resolved by noting that small vacuum resistivities increase the effect of the perturbed current density on the evolution of the corresponding magnetic flux, if we assume the ratio of convection and resistivity term to depend only weakly on η_V . Since

$$(1) \quad J = -\nabla_{\perp}^2 \psi \sim (m^2 + n^2) \psi_{m,n},$$

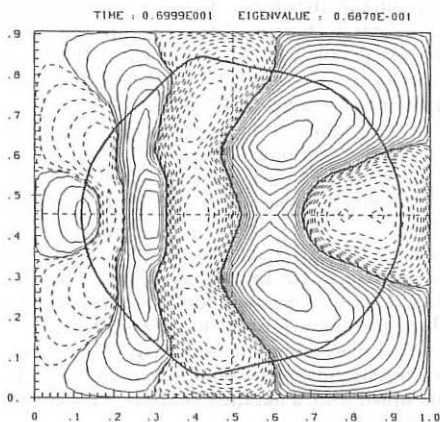


Fig.1

we expect a stronger attenuation of the high- m contributions at the plasma surface compared to the case with large η_V . On the other hand, experimental data suggest a strong insulation between the conducting wall and the plasma surface, since high m -numbers persist close to the vacuum vessel. We therefore increase η_V exponentially from its value at the plasma boundary to a large resistivity near the wall. Furthermore this treatment naturally leads to stronger effects at the inner side of the torus, where the equilibrium magnetic flux is smaller than at the outer side. As can be seen in Fig.1 for the discharge #17005 ($\beta_p \approx 2.1$), this procedure leads to the required large m -values as well as to the correct mode asymmetry.

3. Non-linear results : For a detailed comparison with experiment we have to perform non-linear calculations, which require the superposition of all Fourier components of the expansion in toroidal direction. In practice it turns out that three Fourier components are sufficient. The non-linear evolution is started with the corresponding linear $n = 1$ eigenfunction. Higher n 's will pick up their values by convolution with the $n = 1$ contribution. The amplitudes for the initial eigenfunctions have to be chosen such that the evolution remains in the linear phase for a couple of Alfvén times. Usually, since the Strauss equations in high- β ordering do not lead to a true saturation in the non-linear phase, the evolution is stopped as soon as the calculated perturbed magnetic field at the outboard side of the torus reaches the measured amplitude.

This procedure, however, suffers from the serious drawback that in most of the cases the experimental level is reached when the discharge is still in the linear phase. If, on the other hand, non-linear effects turn out to be strong, they are most likely due to numerical errors caused by a continuously steepened gradient of the perturbed pressure at the outer side of the torus. Thus, for a reasonable comparison with experiment, these calculations are of limited use only.

Since instability, as well as saturation in the non-linear phase are intimately related to the pressure evolution, we introduce a diffusive damping term for the perturbed pressure with a factor linearly dependent on $p_{max} = \max(p(x, y))$, which we consider to be a re-introduction of a numerically not properly treated effective pressure diffusion :

$$(2) \quad \frac{\partial p}{\partial t} = -\vec{v}_{\perp} \cdot \vec{\nabla}_{\perp} p + C p_{max} \nabla_{\perp}^2 p.$$

The constant C is chosen such that the corresponding saturated value for \tilde{B} matches the experimental level. Typically we find $\tilde{B} \sim C^{-1}$.

We note in passing that we have tried alternatively to reduce the pressure steepening by the inclusion of some specific terms of order ϵ^3 , which ensure the correct treatment of the sound wave, i.e. with finite velocity, and lead to an equilibration of the perturbed pressure along lines of constant flux. However, these effects are significant only if the ratio of growth rate $\gamma = \tilde{\gamma}v_A$ and sound velocity v_s satisfies

$$(3) \quad \frac{\gamma}{v_s} = \tilde{\gamma} \frac{v_A}{v_s} = \tilde{\gamma} \frac{B}{\sqrt{\mu_0 \gamma_{HP}}} \ll 1,$$

where $\tilde{\gamma}$ is the normalized growth rate as calculated by the code and v_A the Alfvén velocity. For the parameter values of the discharges under consideration this inequality is not satisfied. The corresponding results predict equilibria to be more unstable by $\sim 30\%$ if the additional terms are taken into account. Therefore these terms do not achieve the non-linear saturation for the presently discussed discharges.

4. Comparison with experiment : Comparisons of numerical results (solid lines) with measurements (circles) are shown in Fig.2a,b for a medium and a large β_p discharge, respectively.

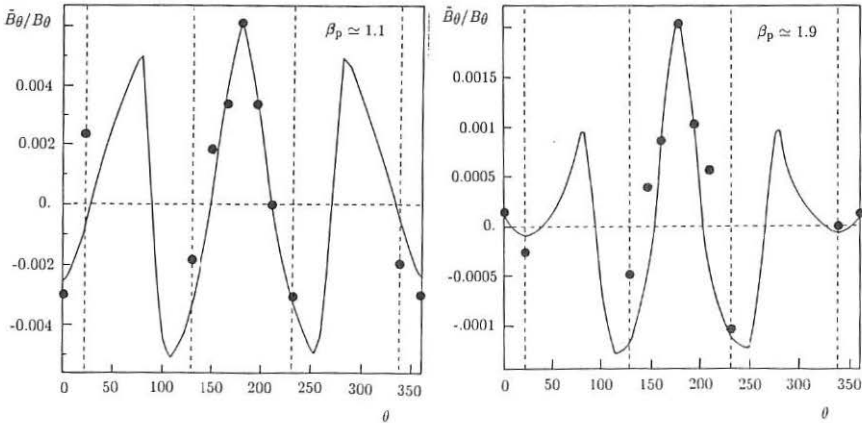
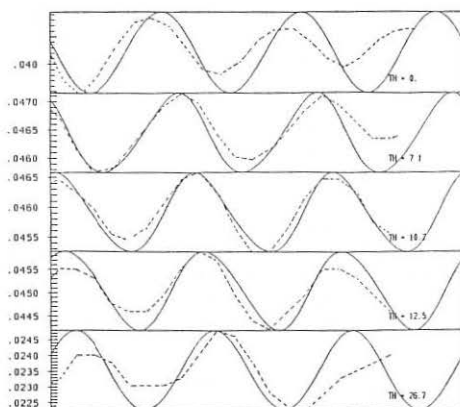


Fig.2a,b

Plotted is the quantity \tilde{B}_θ versus poloidal angle at a fixed toroidal position after saturation in the non-linear phase. Due to the large outside-inside amplitude ratio, nonlinear effects turn out to be stronger at the inner side of the torus.

Note that the vertical dashed lines indicate the limited poloidal range covered by Mirnov probes. This experimental restriction clearly makes a unique determination of the poloidal mode number difficult. However, as can be seen in Fig.2 the comparison with data in the experimentally testable poloidal region shows a reasonable agreement with respect to phases as well as to amplitudes.

The deviation of the observed soft X-ray wave forms from pure $\sim \sin(n\phi)$ can be regarded as a measure of non-linear effects. This offers the possibility to compare our saturation mechanism and thus the corresponding $n > 1$ contributions with data.



In Fig.3 we confront measured soft X-ray traces (dashed lines) versus time for the discharge #18041 with calculations of the line integrated squared perturbed pressure (solid lines) [7]. The missing doubled frequency in the central channel indicates, in agreement with experiment, the weak $m = 1$ contribution. Our results show that the phase differences of the various traces are reproduced to good accuracy. For this special case it turns out that the ratio of $n = 2$ to $n = 1$ contributions is less than 10%.

Fig.3

In summary, global MHD-stability calculations have been carried out for H-mode, high- β_p -ASDEX discharges. It has been shown that at high β_p the discharges are subject to a pressure driven tearing instability, whereas at low β_p the instability is principally of tearing type. When the vacuum resistivity is exponentially increased from its value η_p at the plasma surface to a large value (we have used $\eta_V(max) = 10^{-1}$) near the conducting wall, we find large poloidal mode numbers for the analyzed high- β_p discharges - in agreement with experimental observations.

Non-linear calculations with forced saturation by an effective pressure diffusion term predict amplitudes of non-linear contributions to the $n = 1$ eigenfunctions of the order of 10%. These effects turn out to be stronger at the inner side of the torus, mainly because of the large outside-inside amplitude ratio. Calculations for \tilde{B}_θ versus poloidal angle as well as the line integrated perturbed pressure, which we compare with SXR-data, are in reasonable agreement with experiment.

REFERENCES

1. R. Hawryluk, Physics of Plasmas Close to Thermonuclear Conditions, Vol I, Varenna (1979), (EUR-FU-BRU/XII/476/80).
2. O. Gruber, et al., 13th European Conf. on Controlled Fusion and Plasma Heating, Schliersee 1986, p. 248.
3. O. Klüber, et al., 13th European Conf. on Controlled Fusion and Plasma Heating, Schliersee 1986, p. 136.
4. Lee J.K., Phys. of Fluids **29** (1986), p. 1629; Nucl. Fusion **26** (1986), p. 955.
5. K. Grassie, et al., Inter. Workshop on Turbulence and Anomalous Transport in Magnetized Plasmas, Cargèse 1986, p. 279.
6. O. Gruber, et al., 11th Inter. Conf. on Plasma Physics and Controlled Nuclear Fusion Research, Kyoto 1986.
7. J.L. Dunlap et al., Phys. Rev. Lett. **48** (1982), p. 538.